

Advances in Ceramics for Environmental, Functional, Structural, and Energy Applications II

Edited by

Amar Bhalla

Morsi Mahmoud

Narottam Bansal

Danilo Suvorov

Ruyan Guo

Rick Ubic

Jake Amoroso

Cory Trivelpiece

Navin Manjooran

Gary Pickrell

Dinesh Agrawal

Ceramic
Transactions
Volume 266



WILEY

Advances in Ceramics for Environmental, Functional, Structural, and Energy Applications II

Advances in Ceramics for Environmental, Functional, Structural, and Energy Applications II

Ceramic Transactions, Volume 266

Edited by

Amar Bhalla
Morsi Mahmoud
Narottam Bansal
Danilo Suvorov
Ruyan Guo
Rick Ubic
Jake Amoroso
Cory Trivelpiece
Navin Manjooran
Gary Pickrell
Dinesh Agrawal



WILEY

This edition first published 2019
© 2019 The American Ceramic Society

All rights reserved. No part of this publication may be reproduced, stored in a retrieval system, or transmitted, in any form or by any means, electronic, mechanical, photocopying, recording or otherwise, except as permitted by law. Advice on how to obtain permission to reuse material from this title is available at <http://www.wiley.com/go/permissions>.

The rights of Amar Bhalla, Morsi Mahmoud, Narottam Bansal, Danilo Suvorov, Ruyan Guo, Rick Ubic, Jake Amoroso, Cory Trivelpiece, Navin Manjooran, Gary Pickrell, and Dinesh Agrawal to be identified as the authors of the editorial material in this work have been asserted in accordance with law

Registered Office

John Wiley & Sons, Inc., 111 River Street, Hoboken, NJ 07030, USA

Editorial Office

111 River Street, Hoboken, NJ 07030, USA

For details of our global editorial offices, customer services, and more information about Wiley products visit us at www.wiley.com.

Wiley also publishes its books in a variety of electronic formats and by print-on-demand. Some content that appears in standard print versions of this book may not be available in other formats.

Limit of Liability/Disclaimer of Warranty

In view of ongoing research, equipment modifications, changes in governmental regulations, and the constant flow of information relating to the use of experimental reagents, equipment, and devices, the reader is urged to review and evaluate the information provided in the package insert or instructions for each chemical, piece of equipment, reagent, or device for, among other things, any changes in the instructions or indication of usage and for added warnings and precautions. While the publisher and authors have used their best efforts in preparing this work, they make no representations or warranties with respect to the accuracy or completeness of the contents of this work and specifically disclaim all warranties, including without limitation any implied warranties of merchantability or fitness for a particular purpose. No warranty may be created or extended by sales representatives, written sales materials or promotional statements for this work. The fact that an organization, website, or product is referred to in this work as a citation and/or potential source of further information does not mean that the publisher and authors endorse the information or services the organization, website, or product may provide or recommendations it may make. This work is sold with the understanding that the publisher is not engaged in rendering professional services. The advice and strategies contained herein may not be suitable for your situation. You should consult with a specialist where appropriate. Further, readers should be aware that websites listed in this work may have changed or disappeared between when this work was written and when it is read. Neither the publisher nor authors shall be liable for any loss of profit or any other commercial damages, including but not limited to special, incidental, consequential, or other damages.

Library of Congress Cataloging-in-Publication Data is available.

ISBN: 9781119631484

ISSN: 1042-1122

Cover design by Wiley

Printed in the United States of America.

10 9 8 7 6 5 4 3 2 1

Contents

Preface	ix
ADVANCES IN DIELECTRIC MATERIALS AND ELECTRONIC DEVICES	
Effect of Atmosphere on Dielectric Properties of Calcium Copper Titanate Ceramics	3
Disna P. Samarakoon, Nirmal Govindaraju, and Raj N. Singh	
Integrated Piezoelectric and Thermoelectric Sensing and Energy Conversion	15
Bryan Gamboa, Maximilian Estrada, Albert Djikeng, Daniel Nsek, Shuza Binzaid, Samer Dessouky, Amar S. Bhalla, and Ruyan Guo	
Experimental and Numerical Evaluation of Stacked Piezoelectrics for Mechanical Energy Harvesting	23
Bryan Gamboa, Ruyan Guo, and Amar S. Bhalla	
Temperature Dependent Measurements of Dielectric Properties for Sugary Carbonated Solutions Prepared in Various CO ₂ Pressure Conditions	31
Carlos Acosta, Amar Bhalla, and Ruyan Guo	
Pyrolytic Graphite-Copper Thermocouple for Non-Invasive Direct Temperature Measurement	39
Abdul-Sommed Hadi, Jonathan Lann, Tyler Fricks, and Bryce E. Hill	
Development of Ferroic and Multiferroic Nanomaterials for Drop-on-Demand Microfabrication	49
Brandon D. Young, Bryan Gamboa, Denise Alanis, Luiz Cotica, Amar Bhalla, and Ruyan Guo	

Synthesis of High Curie Temperature $\text{La}_2\text{Ti}_2\text{O}_7$ Piezoceramic by Mechanochemical Activation: A Preliminary Investigation	59
Kaustubh Ramesh Kambale, Ajit R. Kulkarni, Narayanan Venkataramani, Amruta Vairagade, and Sandeep Butee	

INNOVATIVE PROCESSING AND SYNTHESIS OF CERAMICS, GLASSES AND COMPOSITES

Morphological Transition and Evolution of Shapes in Glassy State; Barium Strontium Titanate Dielectric Capacitor Material	69
N. B. Singh, Ching Hua Su, Fow-Sen Choa, Brad Arnold, Lisa Kelly, K. D. Mandal, Narayan Singh, S. Pandey, and Christopher Cooper	

INTERNATIONAL SYMPOSIUM ON CERAMIC MATRIX COMPOSITES

Advanced Environmental Barrier Coatings for SiC CMCs	83
Larry Fehrenbacher, David Kroliczek, Jeffrey Kutsch, Igor Vesnovsky, Erik Fehrenbacher, Anindya Ghoshal, Michael Walock, Muthyvel Murugan, and Andy Nieto	

MATERIALS FOR NUCLEAR ENERGY APPLICATIONS

Density Functional Theory Modeling of Cation Diffusion in Bulk Tetragonal Zirconia	97
Yueh-Lin Lee, Yuhua Duan, Dane Morgan, Dan C. Sorescu, Harry Abernathy, and Gregory Hackett	

Identifying a First Principles Descriptor for Tritium Diffusivities in Lithium Metal Oxides for Tritium Producing Burnable Absorber Rod Applications	111
Yueh-Lin Lee, Caroline Fedele, Hari P. Paudel, Dan C. Sorescu, Yuhua Duan	

Optimizing Processing Conditions for Thorium Dioxide Using Spark Plasma Sintering	121
Anil Prasad, Linu Malakkal, Lukas Bichler, and Jerzy Szpunar	

NANOTECHNOLOGY FOR ENERGY, ENVIRONMENT, ELECTRONICS, HEALTHCARE AND INDUSTRY APPLICATIONS

The Development and Characterization of Mechanically Exfoliated Graphite Based Counter Electrode for Natural Dye Sensitized Solar Cell (DSSC)	135
M.U. Manzoor, M.T.Z. Butt, M.S. Dar, M.H. Ashraf, T. Ahmad, and M. Kamran	

PROCESSING AND PERFORMANCE OF MATERIALS USING MICROWAVES, ELECTRIC AND MAGNETIC FIELDS, ULTRASOUND, LASERS, AND MECHANICAL WORK – RUSTUM ROY SYMPOSIUM

The Effects of Microwave Radiation on the Digestion of Gibbsite by Sodium Hydroxide	143
Ben Dillinger, Carlos Suchicital, David Clark, Andrew Batchelor, Chris Dodds, and Sam Kingman	
Effects of Pore Size and Heating Method on Drying Porous Fused Silica	157
Peter W. Loomis and David E. Clark	
Microstructure and Microtexture of Induction Sintered Copper-based Powder Metal Parts	167
Daudi Waryoba	
Interpreting Non-Thermal Microwave Effects on Materials Process Enhancements – A Straightforward Irreversible Thermodynamic Approach	181
Boon Wong	
Biofilm Formation Behaviors Formed by <i>E.Coli</i> Under Weak Alternating Electromagnetic Fields	195
Hideyuki Kanematsu, Takaya Katsuragawa, Dana M. Barry, Keiya Yokoi, Senshin Umeki, Hidekazu Miura, Koji Suzuki, Akiko Ogawa, Nobumitsu Hirai, Takeshi Kougo, Daisuke Kuroda, and Stefan Zimmerman	

ADVANCES IN ECO-FRIENDLY AND SUSTAINABLE MATERIALS

Evaluation of Durability of Hydraulic Concrete with Colombian Aggregates: An Industrial Byproduct and a Mitigating Addition of The Reaction Alkali-Silica	213
Guilliana Agudelo, Carlos A. Palacio, and Henry A. Colorado	
Mechanical and Physical Characterization of the Natural Fiber <i>Luffa Cylindrica</i> for Its Possible Use in Contact Sports Equipment: 1st Stage	225
Alejandro Restrepo Carmona, and Henry A. Colorado	
Waste Tire Rubber in Calcium Phosphate Cement Blends	237
Carlos F. Revelo, and Henry A. Colorado	
Fabrication by Additive Manufacturing of Clay with Electric Arc Furnace Steel Dust (EAF Dust)	249
Edisson Ordoñez and Henry A. Colorado	

Preface

This volume contains 22 manuscripts presented during the Materials Science & Technology 2018 Conference (MS&T'18), held October 14-18, 2018 at the Greater Columbus Convention Center, Columbus, Ohio. Papers from the following symposia are included in this volume:

- Advances in Dielectric Materials and Electronic Devices
- Innovative Processing and Synthesis of Ceramics, Glasses and Composites
- International Symposium on Ceramic Matrix Composites
- Materials for Nuclear Applications and Extreme Environments
- Nanotechnology for Energy, Environment, Electronics, Healthcare and Industry
- Processing and Performance of Materials Using Microwaves, Electric and Magnetic Fields, Ultrasound, Lasers, and Mechanical Work – Rustum Roy Symposium

These symposia provided a forum for scientists, engineers, and technologists to discuss and exchange state-of-the-art ideas, information, and technology on advanced methods and approaches for processing, synthesis, characterization, and applications of ceramics, glasses, and composites.

Each manuscript was peer-reviewed using The American Ceramic Society's review process. The editors wish to extend their gratitude and appreciation to their symposium co-organizers, to all of the authors for their valuable submissions, to all the participants and session chairs for their time and effort, and to all the reviewers for their comments and suggestions.

We hope that this volume will serve as a useful reference for the professionals working in the field of materials science.

Amar Bhalla
Morsi Mahmoud
Narottam Bansal
Danilo Suvorov
Ruyan Guo
Rick Ubic
Jake Amoroso
Cory Trivelpiece
Navin Manjooran
Gary Pickrell
Dinesh Agrawal

Advances in Dielectric Materials and Electronic Devices

EFFECT OF ATMOSPHERE ON DIELECTRIC PROPERTIES OF CALCIUM COPPER TITANATE CERAMICS

Disna P. Samarakoon, Nirmal Govindaraju, and Raj N. Singh

School of Materials Science & Engineering, Helmerich Advanced Technology Research Center, Oklahoma State University, Tulsa, OK 74106.

ABSTRACT:

The stability and reproducibility of dielectric properties displayed by calcium copper titanate (CCTO) ceramics can be of concern when they are used as capacitor dielectrics and energy storage applications. Highly irreproducible dielectric properties were observed for samples tested in ambient conditions suggesting that ambient played an important role on the stability of dielectric properties. Consequently, the effects of various atmospheric conditions such as air, moisture, and inertness of the atmosphere on dielectric properties were studied on dense and phase pure CCTO samples prepared by powder processing and sintering. Stable and reproducible impedance data were successfully achieved by testing the samples in dry N₂. Especially, low frequency dielectric properties were greatly enhanced in dry ambient than in humid air. This new approach of characterizing dielectric properties of CCTO can be used to eliminate hysteresis due to ambient atmosphere and produce stable and reproducible properties. These results will be presented and discussed.

INTRODUCTION

Solid CaCu₃Ti₄O₁₂ (CCTO) is a perovskite type with a large dielectric constant (ϵ') of 10⁴-10⁵ at room temperature (RT) that is capable of use in supercapacitors [1-3]. CCTO microstructure is electrically heterogeneous composed of semi-conducting grains and insulating boundaries (GBs) [4-6]. Origin of large- ϵ' in polycrystalline CCTO has therefore been widely attributed to barrier layer capacitance effect originated at GBs in [7, 9]. Despite the large- ϵ' , value of dielectric loss ($\tan \delta$) <0.05 over a wide frequency range is still not achieved for CCTO and hence prevent its capacitor applications [10-11].

Synthesis of CCTO with reduced $\tan \delta$ while maintaining its large- ϵ' is a challenge because dielectric properties of CCTO are closely related to its synthesis conditions [12-20] and microstructure [16, 21, 22]. Even when prepared by the same preparation conditions or with small changes in the processing, a wide variations of $\tan \delta$ and ϵ' values were reported for CCTO ceramics. This indicates that this material is still not well characterized to find out the reasons for large variations in its properties.

Our preliminary experiments showed that dielectric properties of CCTO are very sensitive to ambient air atmosphere where the samples were kept while measuring the AC impedance irrespective of the sintering temperatures. In order to reliably use the CCTO materials as capacitors, its surrounding atmosphere dependent dielectric properties are necessary to eliminate or decrease. However, to the best of our knowledge, electrical properties of CCTO ceramics has not been systematically investigated in a controlled atmosphere. This may have led to reported data in the published literature that cannot be fully rationalized.

In the light of these shortcomings, the current study investigated the effect of ambient atmosphere such as air, moisture, and inert conditions on the stability and reproducibility of the electrical properties displayed by CCTO ceramics and thereby eliminating inconsistent dielectric properties of measured samples. This work is a part of long term study on the dielectric properties of CCTO ceramics in both air and in a controlled environment to address these issues. Current

experiments focused on synthesis of CCTO ceramics and characterization microstructures and its dielectric properties.

In the current experiments, the electrical properties such as complex impedance, ϵ' , $\tan \delta$, and DC resistance of the CCTO sample S1070 (sintered for 5 h at 1070°C in air) are measured in both air and dry N₂ atmospheres. Electrical properties are characterized using AC impedance spectroscopy while CCTO samples were kept in controlled ambient air and dry atmospheres as a function of frequency (from 1 Hz to 4 MHz) and temperatures from (23°C to 225°C).

We report highly irreproducible impedance spectra when the samples were kept in air at low temperatures. Interestingly, reproducible impedance spectra with a lowered $\tan \delta$ were seen by switching the atmosphere from air to dry N₂. Data are analyzed and presented with a consideration for more evidence of temperature and frequency dependency of dielectric properties in both the testing atmospheres. The presence of moisture in air and its influence on dielectric loss is also highlighted for observed changes. This study may provide an understanding of the important roles of surrounding atmosphere and sample preparation conditions on the stability of electrical response of polycrystalline CCTO ceramics.

EXPERIMENTAL PROCEDURE

Pure CCTO powder was synthesized by solid-state reaction using stoichiometric ratio of the high-purity CaCO₃ (VWR, 99.95%), CuO (VWR, 99.7%), and TiO₂ (Sigma-Aldrich, Anatase 99.8%) raw materials. Calcination temperature of 850°C for 6 h in air was identified by thermogravimetric analysis (TGA, Netzsch STA 449 F1 Jupiter). Average particle size for all the calcined powders was measured as 500 nm using Malvern Zeta-sizer. Finely ground calcined powders were mixed with 0.5weight % PVB and was uniaxially pressed at 165 MPa into 13 mm diameter and 2.5 mm thick pellets. Additional information on processing can be found elsewhere [23, 24]. Phases present in the calcined powders and sintered sample at 1070°C for 5 h (S1070) in air were identified using X-ray diffraction analysis (XRD, Bruker AXS D8 Discover). Scanning Electron Microscopy (SEM) was used to identify the microstructure of the S1070 whereas density was determined using Archimedes method.

Platinum electrodes were applied on to as-sintered pellets and were thermally cured at 600°C for 2 h. Complex impedance spectra ($Z^* = Z' - jZ''$, where Z' and Z'' are real and imaginary parts) were measured in the frequency range from 1 Hz to 4 MHz with 100 mV AC by an impedance analyzer (Solartron 1260A) and dielectric interface (Solartron 1296). Measurements were carried out at various heat/cool cycles between 23°C and 225°C while keeping the S1070 in both air and dry N₂ atmospheres. Firstly, the complex impedance of as-prepared sample was measured in air atmosphere. Secondly, the measuring environment was shifted by dry N₂ while keeping the ambient pressure of 0.02-0.04 MPa inside the tube furnace. The S1070 was thermally treated by heating up to 400°C in N₂ and evacuating for 30 mins at this temperature and its complex impedance was measured in N₂. Leads/instrument impedance was separately measured and was subtracted from the data before interpretation.

RESULTS

The relative density of the sample S1070 was 4.669 ± 0.042 g/cc (94% of the theoretical density - 5.049 g/cm³). Signs of secondary phase segregation were relatively negligible as observed by XRD for calcined CCTO powders or sintered ceramics in Fig.1.

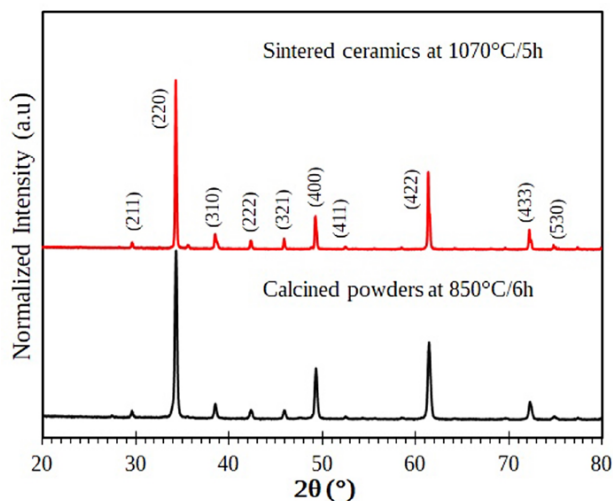


Fig.1. XRD patterns of CCTO calcined powders at 850°C for 6h and sintered ceramics at 1070°C for 5h.

SEM in Fig.2 is the polished surface of the S1070 shows a duplex nature microstructure. Some areas of S1070 microstructure shows no clear boundaries indicating an incomplete grain growth with large sized grains ($<20\ \mu\text{m}$) while large number of smaller grains ($\sim 1\ \mu\text{m}$) segregated at the GBs.

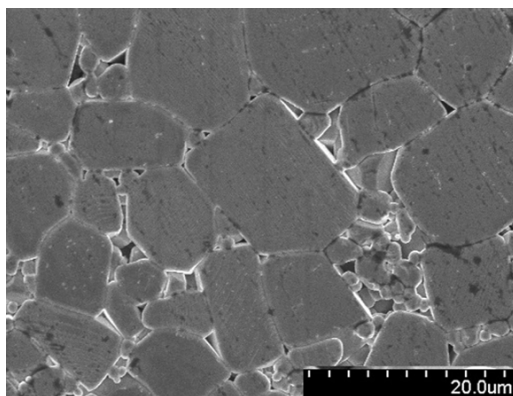


Fig.2. SEM micrograph of polished S1070 surface.

Impedance spectra of the S1070 at 23°C in both air and N_2 are shown in Fig.3 (a) and (b), respectively. As can be seen in Fig.3 (a), in ambient air, there is an inconsistency of the total impedance measured at 23°C (near to RT) at low frequency. However, when the measuring

environment was shifted from air to dry N₂, irreproducibility was eliminated and stable impedance spectra could be seen.

As shown in Fig.3 (b), the arcs related to bulk resistance of S1070, which is implied by the non-zero intercepts at high frequency, are coincident with each other despite the surrounding measuring atmospheres. This suggests negligible impedance change in the bulk of CCTO due to measuring atmosphere. It is also evident that only the low frequency impedance arcs measured in air at 23°C are very sensitive to testing atmosphere. Therefore, GBs and/or electrode sample contact layers seem to play an important role in controlling the complex impedance of CCTO measured in ambient air. After treating in N₂, when the samples were left in air atmosphere and re-measured in air in ambient conditions, impedance spectra were again returned to their unpredictable nature implying the instability when exposed to air atmosphere.

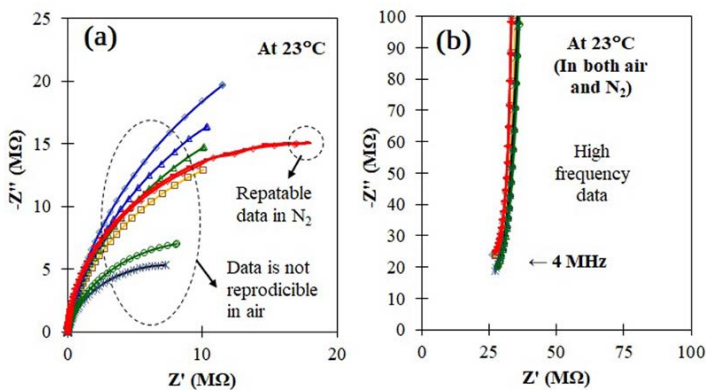


Fig.3. (a) Impedance spectra of the same S1070 measured at 23°C in both air and N₂ atmospheres (b) is the corresponding high frequency data.

Impedance spectra were further explored at high temperature from 23°C to 225°C in both air and N₂ atmospheres. As can be seen in Fig. 4 (a) and (b), fully resolved semicircles were observed for the same S1070 at 58°C and at 89°C, respectively in both air and N₂ atmospheres. The different curves in Fig.4 (a) and (b) are from the measurements done on the same sample repeatedly while heating and cooling cycles in air and N₂ atmospheres. As depicted in Fig.4 (a)-(b), S1070 shows a large deviation and irreproducibility of the total impedance when exposed to air even at higher measuring temperatures compared with the same sample measured in dry N₂. Fully resolved semicircular arcs (not shown here) could be seen for the rest the high temperatures beyond 89°C until 225°C in both the atmospheres with no indication of electrode and sample contact related impedance arcs. Therefore, the impedance data were analyzed using modified Cole–Cole function derived for two parallel RC circuits connected in series to account for grain and GB regions, respectively [25]. DC resistance values were obtained by the intercept on the real axis, which is the diameter of each semi-circle. The capacitance (C) was determined by the maximum of each arc at which $\omega RC=1$, where, $\omega=2\pi f_{\max}$ is the angular frequency and f_{\max} is the peak frequency [25].

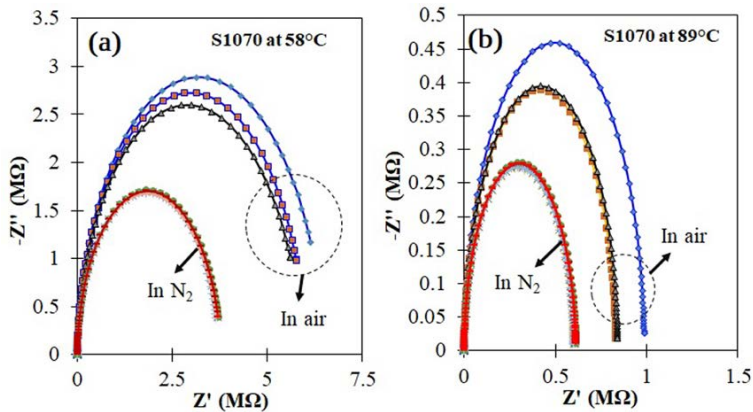


Fig.4. Impedance spectra of the same S1070 measured in both air and N₂ atmospheres at (a) 23°C and at (b) 89°C.

The fitted values obtained for the same S1070 at various temperatures from 23°C to 225°C are shown in Table 1. Grain resistance, GB resistance, and GB capacitance are shown as R_g, R_{gb}, and C_{gb}, respectively. R_{gb} values at 23°C show a range of values in air whereas the same sample measured in N₂ shows a relatively stable value. The total impedance (sum of R_{gb} and R_g) of S1070 measured at 23°C is decreasing rapidly when increasing the temperature to 225°C. Increasing the temperature beyond 114°C the changes were apparently negligible irrespective of the measuring atmosphere.

Increasing the temperature has shifted the peak frequencies to higher frequencies implying the thermal activation of charge carriers. Large GB capacitance can be seen for S1070 at air atmosphere near 23°C. Interestingly, C_{gb} is relatively stable and temperature-independent in N₂ atmosphere at all the temperatures while it is stable in air atmosphere only beyond 89°C suggesting the role of moisture/air on the GB capacitance.

Table 1. Fitted values of grain resistance (R_g), GB resistance (R_{gb}), GB capacitance (C_{gb}), and peak frequencies (f_{max}) in air and N₂ atmospheres at various temperatures (Temp.) for the same CCTO sample S1070.

Temp. (°C)	S1070 in Air				S1070 in N ₂			
	f _{max} (Hz)	C _{gb} (nF)	R _{gb} (Ω)	R _g (Ω)	f _{max} (Hz)	C _{gb} (nF)	R _{gb} (Ω)	R _g (Ω)
23	1	5.2-9.8	(1.4-5.0)E+07	32	1	3.6	(3.1-3.2)E+07	31
58	6	4.5-4.8	(5.9-7.0)E+06	17	6	3.6	3.8.E+06	20
89	52	3.5	(0.8-1.0)E+06	14	43	3.5	(6.0-6.1)E+06	14
114	207	3.4	(2.1-2.6)E+05	10	207	3.5	(1.6-1.7)E+05	11
170	2374	3.5	(1.8-2.1)E+04	5	2374	3.9	1.5.E+04	6
197	7042	3.5	(6.3-6.5)E+03	5	7042	3.7	(6.4-6.5)E+03	5
225	18354	3.5	(2.4-2.6)E+03	4	18354	3.7	2.0.E+02	4

Since we could obtain the repeatable impedance data for S1070 in N_2 atmosphere, DC resistance values of R_g and R_{gb} were further analyzed as a function of temperature. A linear relationship between DC resistance values $\ln(R)$ and $1000/T$ was displayed for S1070 when measured in dry N_2 as shown in Fig.5. The DC conduction activation energy of grain and GBs are shown as E_g and E_{gb} , respectively. A very large resistive behavior of GBs are represented by large activation energies when exposed to N_2 atmosphere. However, grain activation energies are negligibly changed due to atmosphere. GB activation energies are comparable for the typical reported values 0.60 [26] and 0.678 eV [27] for CCTO. Activation energies for intra-grain conduction of this study are also closer to the reported values of 0.08 eV [26] and 0.084 eV [27].

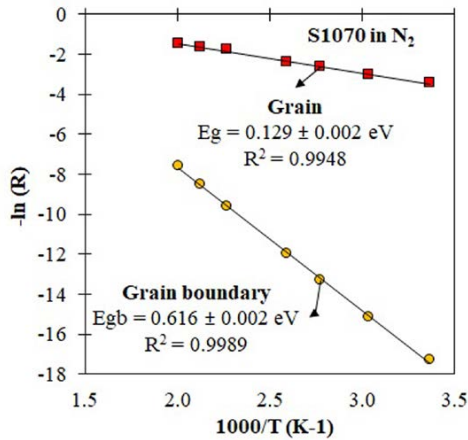


Fig.5. DC resistance of GB and grains in S1070 measured in N_2 as a function of temperature.

Fig.6 (a) and (b), respectively show the ϵ' and $\tan \delta$ measured as a function of frequency in both air and N_2 atmospheres at 23°C. As depicted in Fig.6 (a), there is a strong dispersion with an irreproducible nature of large- ϵ' when S1070 was kept in air. Interestingly, much larger irreproducible nature due to air atmosphere has been effectively suppressed and merged into plateau region from ~100 Hz to 1 MHz when switching the atmosphere from air to N_2 . At frequencies >1 MHz, large- ϵ' of S1070 shows a step-like decrease irrespective of the measuring atmosphere. Still a large- ϵ' can be seen even after switching to N_2 atmosphere without a visible anomaly.

The frequency dependence of $\tan \delta$ exhibits a minimum. Much smaller $\tan \delta$ at 23°C in dry N_2 than in air implies that mobile charges carrier in air atmosphere has been eliminated. As can be seen in Fig.6 (b), upon shifting the measuring atmosphere from air to N_2 , the large dispersion of $\tan \delta$ at low frequencies (< 1 MHz) shows a relatively similar peak heights and shapes, which implies the stability of dielectric losses in N_2 .

For S1070, $\tan \delta$ is less than 0.1 in a wide range of frequencies from 100 Hz to ~100 kHz when exposed to N_2 . However, increase of $\tan \delta$ values can be seen at frequencies >1 MHz and at <100 Hz irrespective of the measuring atmosphere. Loss peak due to bulk relaxation at high frequencies (> 1 MHz) is unchanged despite the atmosphere. This implies that relaxation losses due to bulk of

CCTO are independent of the measuring atmosphere at 23°C while low frequency losses are sensitive to the measuring atmosphere.

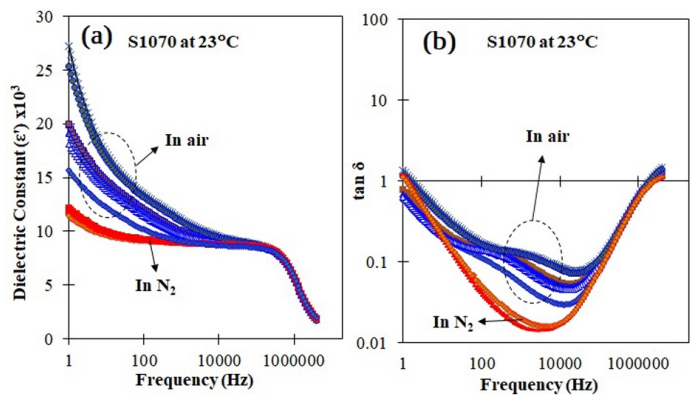


Fig.6. (a) Dielectric constant (ϵ') and (b) $\tan \delta$ for the same S1070 at 23°C in air and N_2 atmospheres.

Table 2 shows the lowest values of $\tan \delta$ with corresponding ϵ' and frequencies for S1070 when exposed to air and N_2 atmospheres. As can be seen in Table 2, frequency at which the lowest $\tan \delta$ is observed has been shifted toward low frequencies while further lowering the values of $\tan \delta$ for S1070 when switching the atmosphere from air to N_2 at 23°C. Upon increasing the temperature from 23°C to 114°C, value of ϵ' related to lowest $\tan \delta$ are relatively stable in N_2 atmosphere compared with the same in air. However, large- ϵ' is retained even at high temperatures (114°C) in both the atmospheres indicating its temperature stability.

Table 2. The lowest values of $\tan \delta$ and corresponding dielectric constants (ϵ') and frequencies for sample S1070 when exposed to both air and N_2 atmospheres.

Temp. °C	tan δ		Dielectric constant (ϵ')		Frequency (kHz)	
	Air	N_2	Air	N_2	Air	N_2
23	0.054 ± 0.016	0.015 ± 0.001	$8,956 \pm 216$	$8,841 \pm 3$	20	4
58	0.015 ± 0.001	0.015 ± 0.000	$8,709 \pm 10$	$8,868 \pm 6$	7.1	6.3
89	0.018 ± 0.000	0.020 ± 0.000	$8,680 \pm 14$	$8,856 \pm 7$	20	20
114	0.027 ± 0.001	0.028 ± 0.000	$8,678 \pm 13$	$8,856 \pm 7$	40	40

DISCUSSION

Moisture absorption from atmospheric air should not be over-looked and could play a key role in controlling the dielectric properties of CCTO. Especially, the stability and reproducibility of dielectric properties displayed by CCTO ceramics is the most important concern, when they are used in capacitors.

Humidity sensitivity of CCTO ceramics is recognized only by limited studies by one group [28, 29], demonstrated that the adsorption of water molecules can affect the potential barrier layer formed at the GBs [28, 29]. Adsorption of moisture on the oxide ceramics surface occurs by the reaction of water molecules with pre-adsorbed oxygen ion by creating surface hydroxyls (OH)

[30-32]. Chemisorbed OH can evolve to water vapor at 300-500°C [30, 31, 33]. Successive layers are physically adsorbed on the OH layer, which may provide the paths to dissolved ions in the air.

The reason for producing reproducible impedance spectra in N₂ in the current experiments can therefore be attributed to the removal of physically adsorbed water due to the thermal treatment of S1070 in dry N₂ to evacuate the water vapor at 400°C. Our experiments showed that there is a definite atmosphere effect on CCTO because when the samples were re-measured in air after treating them in N₂, the unpredictable impedance spectra were again seen for S1070 at RT.

Fitted data show that $R_{gb} \gg R_g$, indicating that highly resistive barrier layers at GBs are dominating the overall DC resistance of the CCTO sample. On the other hand, highly conductive grains in S1070 indicates the presence of sufficient mobile charge carriers in the CCTO lattice [34]. This behavior is consistent with the behavior observed in CCTO ceramics by others [35].

Duplex nature microstructures in S1070 can provide defects such as pores, GBs, which can respond differently to ambient moisture as reported for other humidity sensitive ceramics [36]. A dominant occupancy of large sized conductive grains and islands of smaller grains can provide heterogeneously distributed GBs, which can detour the electric current across the CCTO. When an external AC voltage is passed between conducting grains and insulating GBs, accumulation of charges at the highly resistive GBs can give rise to a large C_{gb} in the structure.

Large- R_{gb} in S1070 despite the atmosphere can be attributed to large number of resistive GBs whereas C_{gb} implies the accumulation of charge carriers at GBs. C_{gb} is related to the effective dielectric constant (ϵ) by $\epsilon = C_{gb}/C_0$, where, C_0 is the vacuum capacitance [37]. In the current experiments, for the same sample thickness with the same grain size, and same electrode material, the nature of absorption moisture in air on the GBs are likely to have an impact on the charge separation. The low frequency dielectric properties of CCTO in the dry N₂ can therefore be associated to the elimination of mobile ion species due to moisture on the GBs and defects.

Some research work indicated a dramatic change of impedance measured near RT when CCTOs were aged in air [14, 38]. However, they haven't reported the data in dry atmosphere [14, 38]. Moreover, studies on both single and polycrystalline CCTO samples indicated a suppression of large- ϵ' in air atmosphere [39-41].

On the contrary, in our experiments, an increased- ϵ' and large $\tan \delta$ due to air atmosphere was seen while a stable and still large- ϵ' with decreased $\tan \delta$ were observed in dry N₂ atmosphere. Increased mobile charge carriers due to humidity in air can increase the electrical conductivity leading to an increased $\tan \delta$ values for the same S1070 [38, 42]. Increasing the surrounding temperature can decrease the atmosphere dependent electrical properties in CCTO because we did not see much larger variation of electrical impedance and GB capacitance beyond 89°C for S1070.

In the current experiments, large- ϵ' and large $\tan \delta$ in air atmosphere can be explained by the relaxation of ionic conductivity associated with the adsorbed moisture on GBs and surfaces. In contact with adsorbed moisture, charge carriers may be free to move resulting in interfacial polarization as we observed in air atmosphere [43]. Removal of moist air and subsequent measurements in dry N₂ can therefore decrease the surface/interface conductivity and can contribute to the reduced $\tan \delta$ and stable large- ϵ' of the present study. The increased- ϵ' due to enhanced ionic and space charge polarization in air atmosphere can on the other hand cause an increased $\tan \delta$ at a given frequency [43].

For the same sample, the existence of low loss and stable- ϵ' at low frequencies (<1 MHz) in N₂ atmosphere could be related to the modification of the conductivity due to removal of ionic species at the insulating GBs. A large and stable ϵ' even in N₂ atmosphere in a large frequency range from 100 Hz to 1 MHz indirectly confirm that sample electrode contact polarization is not the relevant mechanism for large- ϵ' in CCTO.

It is reported for oxide ceramics that even after evacuating the system at 500°C chemically absorbed moisture is difficult to eliminate [30,33]. In the current experiments, a small increase of ϵ' below 100 Hz even in dry N_2 could be attributed either to polarization of chemisorbed moisture, which couldn't be eliminated completely or to electrode sample contact problem.

The results from this study demonstrated that the testing environment needs to be controlled to eliminate hysteresis due to atmospheric effects to obtain stable and reproducible electrical properties in CCTO ceramics. Therefore, we suggest that large discrepancies of dielectric properties reported in the literature for CCTO cannot be solely due to its sensitivity to synthesis conditions but also possibly due to its sensitivity to the ambient humidity.

CONCLUSIONS

In this study CCTO ceramics were synthesized at relatively low calcination temperatures (850°C/6h). Microstructure of sample sintered at 1070°C for 5 h in air (S1070) showed duplex nature. The factors such as testing environment, frequency of the applied electric field, and the temperatures on the electrical properties of S1070 are assessed to find the enhanced dielectric properties. The effect of humidity on the electrical impedance and dielectric properties in two different atmospheres, i.e. air and dry N_2 was measured and compared.

- Highly irreproducible and unpredictable impedance spectra were seen for the same S1070 in air atmosphere at low temperatures (23°C-89°C).
- Reproducible impedance spectra were obtained by switching the atmosphere from air to N_2 after samples were thermally cleaned.
- Fitted reproducible DC resistance values of grains and grain boundaries (GBs) in N_2 atmospheres showed that GBs are highly resistive and possess a large activation energy, which are thermally activated in the temperature range of 23°C and 225°C. Grain activation energy is much low, which reflects the semiconducting nature of CCTO.
- The changes in the large- ϵ' of the sintered sample is caused by the C_{gb} , which is changing due to the differences in charge accumulation when exposed to air or dry N_2 atmospheres.
- For a given sample, an increased C_{gb} at 23°C in air than that in N_2 can be associated with the modification of GBs due to humidity in the air. A clear decrease of $\tan \delta$ values when the air atmosphere was replaced by dry N_2 .
- The same sample indicates much larger minimum value of $\tan \delta \sim 0.1$ in air at 23°C than that in N_2 , which was 0.015 ± 0.001 with ϵ' of $8,841 \pm 3$ at 4 kHz.
- The minima values are relatively unchanged beyond 89°C due to the changes in the measuring atmosphere.

These results suggest that repeatability of electrical properties of the same CCTO sample might be controlled by the sample storage or the pre-treatment atmospheres.

ACKNOWLEDGEMENTS

This project was supported by William's Chair Fund through Oklahoma State University.

REFERENCES

- ¹ R. Schmidt, and D. C. Sinclair, "CaCu₃Ti₄O₁₂ (CCTO) ceramics for capacitor applications," *arXiv preprint arXiv:1402.1621*, 2014.
- ² R. K. Pandey, W. A. Stapleton, J. Tate, A. K. Bandyopadhyay, I. Sutanto, S. Sprissler, and S. Lin., "Applications of CCTO supercapacitor in energy storage and electronics," *AIP Advances*, vol. 3, no. 6, pp. 062126, 2013.

- ³ S. Krohns, P. Lunkenheimer, S. Meissner, A. Reller, B. Gleich, A. Rathgeber, T. Gaugler, H. U. Buhl, D. C. Sinclair, and A. Loidl, "The route to resource-efficient novel materials," *Nature Materials*, vol. 10, pp. 899, 11/23/online, 2011.
- ⁴ T. B. Adams, D. C. Sinclair, and A. R. West, "Giant Barrier Layer Capacitance Effects in $\text{CaCu}_3\text{Ti}_4\text{O}_{12}$ Ceramics," *Advanced Materials*, vol. 14, no. 18, pp. 1321-1323, 2002.
- ⁵ A. A. Felix, M. O. Orlandi, and J. A. Varela, "Schottky-type grain boundaries in CCTO ceramics," *Solid State Communications*, vol. 151, no. 19, pp. 1377-1381, 2011/10/01, 2011.
- ⁶ J.-W. Lee, and J.-H. Koh, "Grain size effects on the dielectric properties of $\text{CaCu}_3\text{Ti}_4\text{O}_{12}$ ceramics for supercapacitor applications," *Ceramics International*, vol. 41, no. 9, Part A, pp. 10442-10447, 2015/11/01/, 2015.
- ⁷ M. A. Subramanian, D. Li, N. Duan, B. A. Reisner, and A. W. Sleight, "High Dielectric Constant in $\text{ACu}_3\text{Ti}_4\text{O}_{12}$ and $\text{ACu}_3\text{Ti}_3\text{FeO}_{12}$ Phases," *Journal of Solid State Chemistry*, vol. 151, no. 2, pp. 323-325, 2000/05/01/, 2000.
- ⁸ C. C. Homes, T. Vogt, S. M. Shapiro, S. Wakimoto, and A. P. Ramirez, "Optical Response of High-Dielectric-Constant Perovskite-Related Oxide," *Science*, vol. 293, no. 5530, pp. 673, 2001.
- ⁹ C. C. Homes, T. Vogt, S. M. Shapiro, W. Si, S. Wakimoto, and M. A. Subramanian, *Charge transfer in the high dielectric constant materials $\text{CaCu}_3\text{Ti}_4\text{O}_{12}$ and $\text{CdCu}_3\text{Ti}_4\text{O}_{12}$* , PHYSICAL REVIEW B, 2002.
- ¹⁰ Y. Li, P. Liang, X. Chao, and Z. Yang, "Preparation of $\text{CaCu}_3\text{Ti}_4\text{O}_{12}$ ceramics with low dielectric loss and giant dielectric constant by the sol-gel technique," *Ceramics International*, vol. 39, no. 7, pp. 7879-7889, 2013/09/01/, 2013.
- ¹¹ L. Singh, U. S. Rai, K. D. Mandal, and N. B. Singh, "Progress in the growth of $\text{CaCu}_3\text{Ti}_4\text{O}_{12}$ and related functional dielectric perovskites," *Progress in Crystal Growth and Characterization of Materials*, vol. 60, no. 2, pp. 15-62, 2014/06/01/, 2014.
- ¹² B. S. Prakash, and K. B. R. Varma, "Influence of sintering conditions and doping on the dielectric relaxation originating from the surface layer effects in $\text{CaCu}_3\text{Ti}_4\text{O}_{12}$ ceramics," *Journal of Physics and Chemistry of Solids*, vol. 68, no. 4, pp. 490-502, 2007/04/01/, 2007.
- ¹³ B. S. Prakash, and K. B. R. Varma, "The influence of the segregation of Cu-rich phase on the microstructural and impedance characteristics of $\text{CaCu}_3\text{Ti}_4\text{O}_{12}$ ceramics," *Journal of Materials Science*, vol. 42, no. 17, pp. 7467-7477, September 01, 2007.
- ¹⁴ M. Li, Z. Shen, M. Nygren, A. Feteira, D. C. Sinclair, and A. R. West, "Origin(s) of the apparent high permittivity in $\text{CaCu}_3\text{Ti}_4\text{O}_{12}$ ceramics: clarification on the contributions from internal barrier layer capacitor and sample-electrode contact effects," *Journal of Applied Physics*, vol. 106, no. 10, pp. 104106, 2009.
- ¹⁵ Y. Wenxiang, "Investigation on the decomposable process and the secondary liquid phase effect on the dielectric properties of $\text{CaCu}_3\text{Ti}_4\text{O}_{12}$ ceramics," *Journal of Physics D: Applied Physics*, vol. 42, no. 17, pp. 175401, 2009.
- ¹⁶ S. Kwon, and D. P. Cann, "Influence of the processing rates and sintering temperatures on the dielectric properties of $\text{CaCu}_3\text{Ti}_4\text{O}_{12}$ ceramics," *Journal of Electroceramics*, vol. 24, no. 3, pp. 231-236, May 01, 2010.
- ¹⁷ L. Pilar, d. I. R. M. A., R. M. Fernando, R. J. José, and F. J. Francisco, "Effect of Processing on the Sintering of High Dielectric constant $\text{CaCu}_3\text{Ti}_4\text{O}_{12}$ Ceramics," *International Journal of Applied Ceramic Technology*, vol. 8, no. 5, pp. 1201-1207, 2011.
- ¹⁸ R. Kashyap, T. Dhawan, P. Gautam, O. P. Thakur, N. Mehra, and R. Tandon, *Effect of Processing Conditions on Electrical Properties of $\text{CaCu}_3\text{Ti}_4\text{O}_{12}$ Ceramics*, 2010.

- 19 T. Adams, D. Sinclair, and A. West, *Influence of Processing Conditions on the Electrical Properties of CaCu₃Ti₄O₁₂ Ceramics*, 2006.
- 20 de la Rubia Miguel A., Leret Pilar, de Frutos Jose, and F. J. F., "Effect of the Synthesis Route on the Microstructure and the Dielectric Behavior of CaCu₃Ti₄O₁₂ Ceramics," *Journal of the American Ceramic Society*, vol. 95, no. 6, pp. 1866-1870, 2012.
- 21 H. Yu, H. Liu, H. Hao, L. Guo, C. Jin, Z. Yu, and M. Cao, "Grain size dependence of relaxor behavior in CaCu₃Ti₄O₁₂ ceramics," *Applied Physics Letters*, vol. 91, no. 22, pp. 222911, 2007.
- 22 L. Ni, X. M. Chen, X. Q. Liu, and R. Z. Hou, "Microstructure-dependent giant dielectric response in CaCu₃Ti₄O₁₂ ceramics," *Solid State Communications*, vol. 139, no. 2, pp. 45-50, 2006/07/01/, 2006.
- 23 D. P. Samarakoon, N. Govindaraju, and R. N. Singh, "Calcium Copper Titanate Based High Dielectric Constant Materials for Energy Storage Applications," *Processing, Properties, and Design of Advanced Ceramics and Composites*, vol. 259, pp. 131, 2016.
- 24 D. P. Samarakoon, N. Govindaraju, and R. N. Singh, "Influence of Processing and Microstructure on Dielectric Properties of Calcium Copper Titanate Ceramics," *Processing, Properties, and Design of Advanced Ceramics and Composites II*, vol. 261, pp. 237, 2017.
- 25 J. R. Macdonald, and E. Barsoukov, "Impedance spectroscopy: theory, experiment, and applications," *History*, vol. 1, no. 8, 2005.
- 26 D. C. Sinclair, T. B. Adams, F. D. Morrison, and A. R. West, "CaCu₃Ti₄O₁₂: One-step internal barrier layer capacitor," *Applied Physics Letters*, vol. 80, no. 12, pp. 2153-2155, 2002.
- 27 J. L. Zhang, P. Zheng, C. L. Wang, M. L. Zhao, J. C. Li, and J. F. Wang, "Dielectric dispersion of CaCu₃Ti₄O₁₂ ceramics at high temperatures," *Applied Physics Letters*, vol. 87, no. 14, pp. 142901, 2005.
- 28 M. Li, "Study of the humidity-sensing mechanism of CaCu₃Ti₄O₁₂", *Sensors and Actuators B: Chemical*, vol. 228, no. 2, pp. 443-447, 2016.
- 29 M. Li, X. L. Chen, D. F. Zhang, W. Y. Wang, and W. J. Wang, "Humidity sensitive properties of pure and Mg-doped CaCu₃Ti₄O₁₂," *Sensors and Actuators B: Chemical*, vol. 147, no. 2, pp. 447-452, 2010/06/03/, 2010.
- 30 E. W. Thornton, and P. G. Harrison, "Tin oxide surfaces. Part 1.-Surface hydroxyl groups and the chemisorption of carbon dioxide and carbon monoxide on tin(IV) oxide," *Journal of the Chemical Society, Faraday Transactions 1: Physical Chemistry in Condensed Phases*, vol. 71, no. 0, pp. 461-472, 1975.
- 31 M. Egashira, M. Nakashima, S. Kawasumi, and T. Selyama, "Temperature programmed desorption study of water adsorbed on metal oxides. 2. Tin oxide surfaces," *The Journal of Physical Chemistry*, vol. 85, no. 26, pp. 4125-4130, 1981/12/01, 1981.
- 32 C. Mrabet, N. Mahdhi, A. Boukhachem, M. Amlouk, and T. Manoubi, "Effects of surface oxygen vacancies content on wettability of zinc oxide nanorods doped with lanthanum," *Journal of Alloys and Compounds*, vol. 688, pp. 122-132, 2016/12/15/, 2016.
- 33 Y. Shimizu, H. Arai, and T. Seiyama, "Theoretical studies on the impedance-humidity characteristics of ceramic humidity sensors," *Sensors and Actuators*, vol. 7, no. 1, pp. 11-22, 1985/03/01/, 1985.
- 34 N. Lei, and C. X. Ming, "Enhancement of Giant Dielectric Response in CaCu₃Ti₄O₁₂ Ceramics by Zn Substitution," *Journal of the American Ceramic Society*, vol. 93, no. 1, pp. 184-189, 2010.

- 35 Z. Guozhong, Z. Jialiang, Z. Peng, W. Jinfeng, and W. Chunlei, "Grain boundary effect on the dielectric properties of $\text{CaCu}_3\text{Ti}_4\text{O}_{12}$ ceramics," *Journal of Physics D: Applied Physics*, vol. 38, no. 11, pp. 1824, 2005.
- 36 Y. C. Yeh, and T. Y. Tseng, "Humidity-sensitive electrical properties of $\text{Ba}_{0.5}\text{Sr}_{0.5}\text{TiO}_3$ porous ceramics," *Journal of Materials Science Letters*, vol. 7, no. 7, pp. 766-768, July 01, 1988.
- 37 J. Liu, C.-g. Duan, W. N. Mei, R. W. Smith, and J. R. Hardy, "Dielectric properties and Maxwell-Wagner relaxation of compounds $\text{ACu}_3\text{Ti}_4\text{O}_{12}$ ($\text{A}=\text{Ca}, \text{Bi}_{2/3}, \text{Y}_{2/3}, \text{La}_{2/3}$)," *Journal of Applied Physics*, vol. 98, no. 9, pp. 093703, 2005.
- 38 E. Schlömann, "Dielectric Losses in Ionic Crystals with Disordered Charge Distributions," *Physical Review*, vol. 135, no. 2A, pp. A413-A419, 07/20/, 1964.
- 39 P. Lunkenheimer, R. Fichtl, S. G. Ebbinghaus, and A. Loidl, "Nonintrinsic origin of the colossal dielectric constants in $\text{CaCu}_3\text{Ti}_4\text{O}_{12}$," *Physical Review B*, vol. 70, no. 17, pp. 172102, Nov, 2004.
- 40 S. Krohns, P. Lunkenheimer, S. G. Ebbinghaus, and A. Loidl, "Broadband dielectric spectroscopy on single-crystalline and ceramic $\text{CaCu}_3\text{Ti}_4\text{O}_{12}$," *Applied Physics Letters*, vol. 91, no. 2, pp. 022910, 2007.
- 41 S. Krohns, P. Lunkenheimer, S. G. Ebbinghaus, and A. Loidl, "Colossal dielectric constants in single-crystalline and ceramic $\text{CaCu}_3\text{Ti}_4\text{O}_{12}$ investigated by broadband dielectric spectroscopy," *Journal of Applied Physics*, vol. 103, no. 8, pp. 084107, 2008.
- 42 A. K. Jonscher, "Dielectric relaxation in solids," *Journal of Physics D: Applied Physics*, vol. 32, no. 14, pp. R57, 1999.
- 43 A. J. MOUNTVALA, "Effect of Surface Moisture on Dielectric Behavior of Ultrafine BaTiO_3 Particulates," *Journal of the American Ceramic Society*, vol. 54, no. 11, pp. 544-548, 1971.

INTEGRATED PIEZOELECTRIC AND THERMOELECTRIC SENSING AND ENERGY CONVERSION

Bryan Gamboa¹, Maximilian Estrada^{1,2}, Albert Djikeng¹, Daniel Nsek^{1,2}, Shuza Binzaid,¹ Samer Dessouky³, Amar S. Bhalla^{1,2} and Ruyan Guo^{1,2,*}

¹Multifunctional Electronic Materials and Devices Research Lab, Department of Electrical and Computer Engineering

²Interdisciplinary Graduate Program in Advanced Materials Engineering

³Department of Civil and Environmental Engineering
University of Texas at San Antonio, San Antonio, TX 78249

ABSTRACT

An integrative approach is carried out utilizing piezoelectric and thermoelectric device sciences, computational modeling and engineering design/testing. Numerical FEA simulation is used extensively to guide the frequency dependent transducer design, device fabrication and power electronics conversion. The research is to develop modular hybrid integrated sensing and energy conversion (HISEC) unit with optimized energy density and power efficiency. While electric power converted from roadways by a single unit (occupying an area of less than 0.1 m²) using piezoelectric or thermoelectric mechanism alone, is considered intermittent or inadequate for intended applications, the energy conversion integrations make it possible to have complementary and parallel modes of energy-harvesting from roadways to have a self-sustained power source that supports sensing and data transmission functions. The evaluation and testing results obtained validated the design concept and are the base for further optimizations. The HISEC module developed is independent of the power grid and with on-demand data monitoring and information transmitting capabilities, thus could play an enabling role in applications such as smart-roadways and smart-cities.

1. INTRODUCTION

Vehicles and semi-trucks commute on roadways 24 hours a day and 7 days a week throughout of the year. The weight of these vehicles puts tremendous stress onto the roads as the wheels pass and produce pressure waves that propagate and dissipate into the pavement. The presence of these waves can potentially be harvested for usable energy if a stress-responsive material is located on or beneath the surface of the road. The most attractive choice of such materials are piezoelectric (PZT in this case) ceramics that convert compressive mechanical stresses into electrical energy. Multiple transducer designs have been evaluated to determine the best candidate for mechanical to electrical energy conversions.

The Texas environment can reach temperatures in excess of 110 degrees Fahrenheit during summer and around freezing during the winter. The surface of the roadway has a substantially different temperature than the ground a few inches below the surface. The presence of this temperature gradient allows for the possibility of harvesting energy from the difference in temperature. Such materials that convert thermal gradients into usable electrical energy are known as thermoelectric generators (TEG; in this case Bi₂Te₃). In the thermoelectric (TE) effect, heat is converted into electrical energy based on the Seebeck effect, which is a constant temperature difference on two sides of dissimilar metals or semiconductors that can produce a steady electric current in a circular loop

*contact email: ruyan.guo@utsa.edu